

Image Enhancement of Motion Blur Based on Chaos Quantum Algorithm

Yanyan Zhou*

School of Mathematics and Computer, Tongling University, Tongling 244000, China

The enhancement of motion-blurred images requires a local optimization solution; hence, a method based on the Chaos Quantum algorithm is designed. The degradation and noise functions are superposed to obtain the degraded image, the quantum particles are updated in the chaotic system, the adaptive denoising algorithm is used to denoise the moving image, the two-stage strategy and popular sorting are used to segment the moving fuzzy image, and the moving image is reconstructed by the chaotic quantum algorithm to improve the moving fuzzy image. The experimental results show that under the influence of strong noise, it has a higher peak signal-to-noise ratio, and the contrasts and details in the image are significantly improved. Compared with the original image, the standard deviation and information entropy of the enhanced image are significantly improved, which shows that the proposed method performs well and can make a significant improvement to motion-blurred images.

Keywords: Chaos Quantum algorithm, motion-blurred image, enhance, noise, degradation

1. INTRODUCTION

The details in images are an important source of information for humans. An image is obtained by observing the objective world in different forms and by means of various observation systems. With the advent of the digital era, image technology has penetrated all aspects of human life and social development. In a broad sense, image technology refers to all kinds of technologies related to image. Imagery technology can be divided into: image processing, image analysis and image understanding. Of these, image processing technology is the most basic and the most important operational step on which subsequent high-level operations are based. Image enhancement is one of the most basic methods of digital image processing. It has two main purposes: to improve the visual effect of the image and improve the clarity of the image components; and secondly, to transform the image into a form more suitable for human observation or automatic computer analysis (Nawaz et al., 2019). In the space docking task, the

captured space moving image is often disturbed by noise and the visual resolution quality is poor, which results in the loss of some motion details. Therefore, it is necessary to obtain an efficient adaptive denoising algorithm to achieve high-quality space image enhancement. The existing denoising methods often blur the details at the edges of the image when the noise is filtered at the same time. In order to achieve more effective spatial image denoising, two difficult problems need to be addressed: How to establish a cross-scale feature description of spatial image in order to obtain a sharper image edge and preserve the details; and how to establish an efficient cross-scale adaptive algorithm to achieve denoising simultaneously. Therefore, image enhancement is a very important issue in image preprocessing, and is a technology with important practical value.

Although there are no specific algorithms for image enhancement, there are many other algorithms that serve different purposes. These algorithms can be divided into “space domain” and “frequency domain” depending on the processing space. There are two processing strategies: global

*Email of Corresponding Author: zyyz014@163.com

image enhancement and local image enhancement. The spatial domain method applies the direct operation of image pixels, which is basically based on the mapping of gray-scale transformation. It is divided into two categories: point processing and neighborhood processing. Point processing is the point-to-point operation of an image, such as image gray-scale transformation, histogram equalization, pseudo color processing, etc. The neighborhood processing operation in the spatial domain is also known as ‘local operation’, such as linear, nonlinear smoothing and sharpening. The frequency domain processing technology is based on the Fourier transform of the modified image, which is used to modify the image transform by means of the filter function, and then obtain the processed output image by the inverse transform of the result. Common processing methods include high and low-pass filtering, homomorphic filtering, and so on. At present, there is no unified and authoritative definition of image enhancement theory (method), and there is no common standard for measuring image enhancement quality. Image quality evaluation is a highly intuitive process. In the research on digital image processing, the spatial domain method can be used only in some specific environments (such as image edge detection or filtering), the universality of the algorithm is poor. The frequency domain processing method usually involves a large number of calculations, and the selection of transformation parameters requires greater manual intervention, which has the problem of producing a low peak signal-to-noise ratio of image.

To address the aforementioned problems, a method based on Chaos Quantum algorithm is designed for the enhancement of motion-blurred images. The chaotic quantum system adapts to the degraded image, and the enhancement of motion blur image is achieved by means of adaptive analysis, two-stage strategy and popular sorting segmentation. The validity of the method is verified by experiments.

2. DESIGN OF IMAGE ENHANCEMENT METHOD OF MOTION BLUR BASED ON CHAOS QUANTUM ALGORITHM

Because there is a certain amount of uncertainty surrounding the behavior of basic particles in quantum mechanics, a quantum unit will have more than two Superposition States, so the amount of information it carries will be far greater than the binary code. The regularity of chaos enables the new solution to be generated by definite iteration; the randomness prevents the search from being trapped into local optimum; the ergodicity makes the final solution approach the real optimal solution with arbitrary precision.

2.1 Chaotic Quantum System

The blurring of images can occur when the image is being taken. Due to the relative motion between the target scene and the imaging equipment, the object in the image is distorted, or the imaging system itself is moving. In any event, the photos taken may be blurred, known as ‘motion blur’.

The degradation is due to the CCD mechanism made up of complex electronic sensor components that respond to the exposure time. In the linear operation analysis of the image, an image is comprised of countless tiny pixels, while the point source is the pixel of the combined image (Eygeny et al., 2017; Rasid et al., 2019), and infinitely many point sources combine to form a clear image. Each pixel is also called a point source. In the mathematical operation, the point source can be represented by Dirac function φ , which is defined as:

$$\varphi(x, y) = \begin{cases} \delta, & x = 0, y = 0 \\ 0, & \text{else} \end{cases} \quad (1)$$

$\varphi(x, y)$ of them need to meet:

$$\int_s^q \int_i^m p\varphi(x, y) = 1 \quad (2)$$

Dirac function φ has the following properties:

First, φ functions are even functions, represented by $\varphi(-x, -y) = \varphi(x, y)$;

Second, separability $\varphi(x, y) = \varphi(x)\varphi(y)$;

When the input is unit pulse $\varphi(x, y)$, the output of the system is called pulse response, which is expressed by two-dimensional function $h(x, y)$; $h(x, y)$ which is regarded as the response to the point source, that is, the point spread function.

According to the above process, the degradation function is obtained. In the degradation of a motion-blurred image, the degradation function and noise function are superposed to generate a motion-blurred image $g(x, y)$, and the fuzzy image is generated with reference to RGB color space (Laparra et al., 2017; Ahmad Khan et al., 2017; Li et al., 2017), as shown in Figure 1.

The process of image degradation can be represented by the following mathematical model:

$$g(x, y) = \int_a^e q(vs, a) \int g + n(x, y) \quad (3)$$

In the formula, $g(x, y)$ represents the motion-blurred image that can be observed from the degraded image; $\int_a^e q(vs, a)$ represents the point spread function; $n(x, y)$ represents the original image that has not been degraded; $\int g$ represents the additive noise introduced in the formation of the motion-blurred image. According to the degraded image, let the quantum particles update in the chaotic system as follows:

$$f_1(x) = \begin{cases} 1 - \sqrt{1 - 2x}, & 0 \leq x \leq \frac{1}{2} \\ \sqrt{1 - 2x}, & \frac{1}{2} \leq x \leq 1 \end{cases} \quad (4)$$

2.2 Moving Image Denoising

In the aforementioned quantum particle chaos system, the cross-scale adaptive denoising algorithm is used to filter the noise and maintain the edge details of the image more effectively. Assuming that y represents noisy spatial image, s represents noise interference, and x represents noiseless

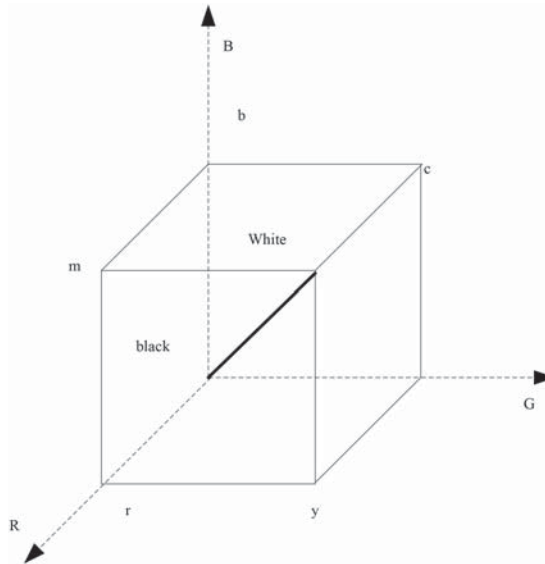


Figure 1 RGB color space.

spatial image, the imaging model of noiseless spatial image can be formalized as:

$$y = x + s \quad (5)$$

There are many kinds of noises in the spatial moving image captured by the vision sensor. The denoising algorithm in this paper applies Gaussian white noise according to the Gaussian distribution (Amid et al., 2017; Thiebaud et al., 2017; Somkuwar et al., 2017; Maleki et al., 2017; Ennis et al., 2018), at the same time, the experimental test is carried out using the combined Poisson noise and the Poisson Gaussian noise model.

In order not to lose generality, the noise here is assumed to be Gaussian white noise. The calculation formula is:

$$\int_a^e q(vs, a) = q(vs, a), \varpi(x, y) \in \Omega \quad (6)$$

In the formula, ϖ and Ω represent the point spread function and the support region of the image respectively.

In this study, the object of the motion deblurring is the digital image, so the above formula can be discretized:

$$g = \sum_{i=1}^e q + b \quad (7)$$

In the formula, g represents the degraded image; $\sum_{i=1}^e q$ represents the original image without degradation; b represents the column vector of additive noise.

When a motion-blurred image is formed, different components of the image may have different motion paths, that is, integral paths. In this case, it is necessary to segment the image, divide the parts using the same motion law, and then to each motion-blurred image with the same PSF.

The purpose of establishing a cross-scale feature description of image by multi-scale geometric analysis method is to eliminate the down sampling operation of image, and to realize different scale decomposition and direction sub-band decomposition of the image by using non-down-sampling

multi-level tower decomposition and non-down sampling, multi-level direction filter bank.

First, we use multi-scale decomposition to obtain different frequency scales. Then we use directional filtering to decompose the high-frequency scales into different directional sub-bands. There can be any number of directional sub-bands. The core structure of the transform is a two-channel non-down sampling filter bank, which satisfies the following equation:

$$H_0(Z)G_0(Z) + H_1(Z)G_1(Z) = \sum_{l=1}^A d \quad (8)$$

In the formula, $H_0(Z)$ and $G_0(Z)$ represent low-pass and high-pass analysis filters respectively; $H_1(Z)$ and $G_1(Z)$ represent low-pass and high-pass synthesis filters respectively.

The schematic diagram of image conversion frequency band decomposition is:

The equivalent filter for the layer decomposition of signals is obtained with:

$$Hz = \begin{cases} H(s^q) \prod_s^e w, 1 \leq l \leq 2 \\ \prod_{j=0}^a dH, l = 2 \end{cases} \quad (9)$$

In the formula, $H(s^q)$ represents high pass filter, $\prod_s^e w$ represents low-pass filter, and convolute the signal with the corresponding filter to obtain multi-scale analysis of the image.

In order to retain more details of the image after denoising, further denoising is carried out. The calculation formula is:

$$w(i, d) = \begin{cases} \sum_d^q(i, d), r \in HF \\ W(i, d), P(I, D) \\ W(i, d), sf \in s \\ W(i, d), W(i, d) \in d_u \end{cases} \quad (10)$$

In the formula, $w(i, d)$ is the domain transform coefficient, $\sum_d^q(i, d)$ is the transform coefficient after de-noising, HF

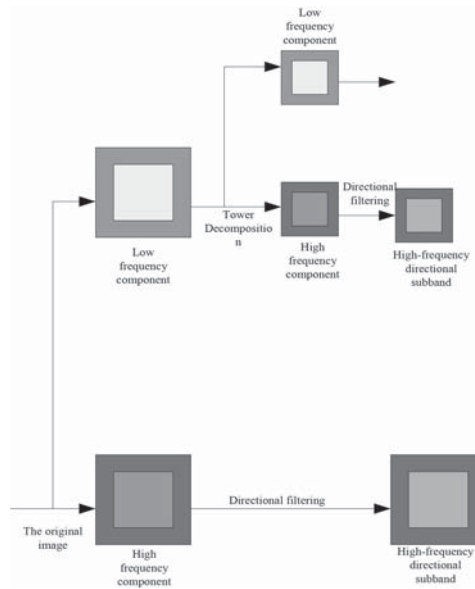


Figure 2 Schematic diagram of frequency band decomposition of image transformation.

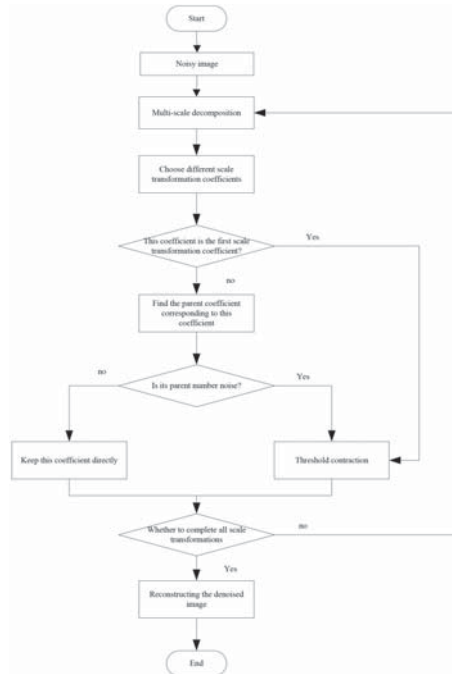


Figure 3 Calculation flow of adaptive denoising algorithm.

is the linear parameter, and sf is the adaptive de-noising function.

The calculation process of the adaptive denoising algorithm is shown in Figure 3.

2.3 Moving Image Segmentation

A super-pixel closed-loop graph is constructed where each node represents a local block area of the image, E represents the edge between two nodes, and its weight is measured by matrix $w = [R_{ij}]$. The formula is:

$$R_{ij} = \sum_a d / \frac{r}{q} \tag{11}$$

In the formula, q, r represent the mean value of the two super pixel nodes in the color space, and $\sum_a d$ represent the constant controlling the weight intensity.

In the graph model, the two-stage strategy and popular sorting are used to detect the significant target area from bottom to top. In the first stage, the nodes in the four boundary regions of the image are selected as the seed nodes of the non-target region (background region), and all other nodes are sorted by similarity, so as to construct four saliency graphs S_q, S_t, S_d, S_a . Then, we combine them to obtain the final saliency graph. After selecting the upper boundary node as the seed node, we obtain the index vector. The calculation method is:

Table 1 Extraction content of target area.

Content	Method	Extract Content
Content 2	Compressed sensing theory	The obtained low-dimensional compressed subspace
Content 3	Sparse measurement matrix	Preserve the information of the original high-dimensional feature space
Content 4	Prospect	Dimensionality reduction
Content 5	Features of the background	Dimensionality reduction
Content 6	Classifier training	Positive and negative examples
Content 7	Naive Bayes classifier predicts target image for next frame	Determine the location of the target area

$$f = (d - hj)_i \quad (12)$$

In the formula, hj is the weight matrix and d is the normalized parameter.

The formula above gives the final visual saliency map with the seed node of the non-target area as the prior. In the second stage, the seed nodes of the target region (foreground region) are selected, and all other nodes are sorted by similarity to further improve the accuracy of significance detection. Firstly, an adaptive threshold is used to segment the first-stage saliency image. In order to ensure that the selected seed cover a greater area, the threshold is determined as the average significance of the whole saliency map. Once the significance seed node is selected, it is obtained by normalization using the formula:

$$S(i) = \sum_d^s fi, i = 1, 2, \dots, n \quad (13)$$

In the formula, $S(i)$ represents the saliency map obtained by seed points in the final target area; $\sum_d^s f$ represents the binary segmentation parameters.

Based on obtained visual saliency map, binary segmentation is carried out to determine the visual saliency area after spatial domain analysis.

Following visual saliency detection, temporal and spatial saliency detection and extraction are realized by combining the motion sequence information of the moving image in the time domain. In this paper, a new real-time tracking mechanism based on compressed sensing is used to extract the time-domain motion saliency target area. The contents are in Table 1 (Mourard et al., 2017; Ofner et al., 2017; Mohammadzade et al., 2017; Khajavi et al., 2017; Eirik et al., 2018; Ramos et al., 2017).

The multi-scale rectangular filter defined by the above formula is convoluted to realize multi-scale transformation, so as to obtain the multi-scale feature vector of each image block. The formula is:

$$h(x, y) = \begin{cases} 1, & 1 \leq x \leq i, 1 \leq y \leq j \\ 0, & d \end{cases} \quad (14)$$

In the formula, i and j are the width and height of the rectangular filter respectively.

The final detection and extraction of spatiotemporal significant moving target area can be realized by combining the

target area obtained from spatial domain analysis and time domain analysis as above. The formula:

$$df = \sqrt{d(i)} / \frac{D}{N} \quad (15)$$

In the formula, df represents the significant moving target area of each image in the image sequence; $d(i)$ represents the parameters of the updated classifier; $\frac{D}{N}$ represents the accuracy of detection and tracking of the significant target area.

2.4 Resolution Reconstruction of Motion-Blurred Image

In the proposed super-resolution reconstruction process, the chaos quantum algorithm is used to reconstruct it. The reconstruction framework is shown in Figure 4 below.

The initial estimation is used to calculate the weight of the first iteration of the reconstruction algorithm. After one iteration, a better high-resolution estimation can be obtained, and then the new estimation can be used to calculate the weight in the next iteration. In order to obtain higher reconstruction quality, this iterative process needs to be repeated many times, and the weight calculation in each iterative process depends on the reconstruction results obtained from the previous iterative process. The performance of the initial high-resolution estimation method directly affects the subsequent super-resolution reconstruction process. The interpolation mechanism based on iterative curvature is used to obtain the initial high-resolution estimation of each low-resolution moving image. The mechanism based on second derivative continuity and energy curvature is not only simple and effective in avoiding a fuzzy or sawtooth effect, but also has real-time performance. In this mechanism, the initial energy value of each interpolation pixel is calculated with:

$$Y = \frac{\sum_x a}{\sum_a w} / r \quad (16)$$

In the formula, Y represents the number of frames in the moving image sequence; $\sum_a w$ represents the low-resolution input sequence; $\sum_x a$ represents the high-resolution output sequence after iterative reconstruction; r is the upper sampling factor.

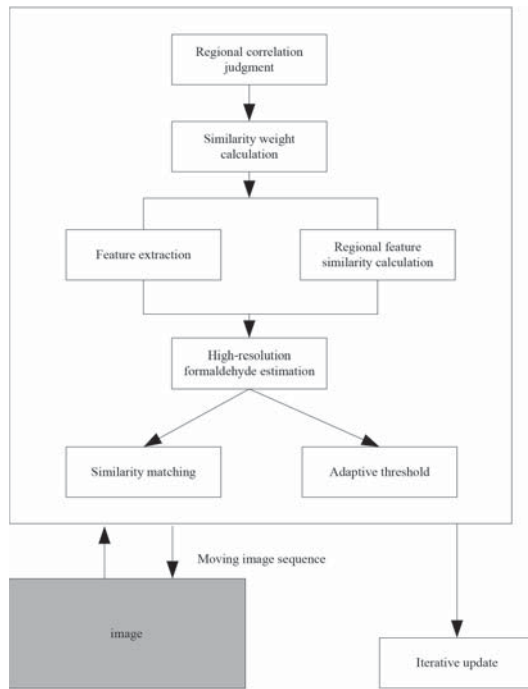


Figure 4 Resolution reconstruction framework of motion-blurred image.

Table 2 Contents of initial value correction

Feature points	Content	Detailed Description
Feature point 1	Define transformation function to adjust the probability of occurrence of quantum ground state	Macro and micro characteristics of edge contours
Feature point 2	Forced inner product constraint in quantum measurement vector	Quantum contour model
Feature point 3	Use non-orthogonal projection instead of orthogonal projection	Morphological structural element description
Feature point 4	Spatiotemporal characteristics of combined spatial moving images	No need to be restricted by physical laws and constraints
Feature point 5	Multi-frame moving image information using different spatiotemporal scales	Signals mapped into quantum space
Feature point 6	Non-local similarity complementary redundant information	Obtained initial high-resolution estimates
Feature point 7	Blends information between shouting moving images	Amount of detail

Whether it is an accurate image registration or a fuzzy registration mechanism, we need to fully consider the translation, rotation and scale invariant characteristics of the image to ensure high-quality reconstruction effect. Therefore, for the initial value correction, the correction contents are in Table 2.

The reconstruction algorithm based on nonlocal similarity can achieve effective super-resolution reconstruction without relying on accurate sub-pixel motion estimation, and can weaken the influence of multiple independent moving objects in the reconstruction process. However, when some objects are missing or there are different rotation angles in the low-resolution sequence image, the correlation and similarity between the frames will be weaker. In this case, the algorithm

cannot make full use of the similar information between the low-resolution images to achieve effective reconstruction. For this reason, the region correlation judgment and adaptive threshold strategy are used for calculation. It is assumed that the image is an 8 * 8 original gray-scale image, and the horizontal and vertical coordinate identification of each pixel is shown in the figure (Yang et al., 2017; Zhang et al., 2017; Christoph et al., 2018; Bao et al., 2018; Hai et al., 2019).

$$Y = \frac{\sum_x a}{\sum_a w} / r \tag{17}$$

In the formula, Y represents the number of frames in the moving image sequence; $\sum_a w$ represents the low-resolution input sequence; $\sum_x a$ represents the high-resolution output



(a) Image 1

(b) Image 2

Figure 5 Experimental image.

sequence after iterative reconstruction; r is the upper sampling factor.

Subsequently, the steps of resolution reconstruction of Motion-Blurred image are as follows:

- Step 1: Input low resolution moving image sequence;
- Step 2: Output the reconstructed high-resolution moving image sequence;
- Step 3: Preprocessing to obtain the initial high-resolution estimation of moving image sequence;
- Step 4: Moment feature extraction is the moment feature vector corresponding to the local block area centered on the pixels to be reconstructed and the forces of each low-resolution pixel;
- Step 5: Adaptive threshold calculation;
- Step 6: Extract the low-resolution area, for which the formula is:

$$D(b) = t * \frac{q}{d/u} \quad (18)$$

In the formula, $D(b)$ represents the size of each frame; t represents the time complexity of the initial estimation stage; d/u represents the parameters of the cross-scale super-resolution reconstruction stage; q represents the number of consecutive frames of reconstruction.

Step 7: Weight accumulation: for each accumulated area above, update the weight.

After following the above process, the reconstruction of the moving image is completed, and finally the image is enhanced.

The process is:

- Step 1: The input image is normalized;
- Step 2: According to the chaos quantum algorithm, the moving image points are optimized. The calculation formula is:

$$f(n) = \sum_{i=1}^d a/h \quad (19)$$

In the formula, $f(n)$ is the fitness function, $\sum_{i=1}^d a$ is the gray distribution parameter after image enhancement, and h is the image contrast function.

- Step 3: The above steps are updated iteratively to meet the fitness function conditions and terminate the iteration;
- Step 4: Anti normalization processing, output image.

3. EXPERIMENTAL DEMONSTRATION

3.1 Experiment Content

In order to verify the effectiveness of the image enhancement method based on the Chaos Quantum algorithm, several experiments are conducted. Utilizing MATLAB 7.0 programming, the hardware platform is CPU 3.6ghz, memory 2048MB, hard disk sata 2.0 interface, and the operating system is window XP. The traditional method is compared with the proposed method (Mohan et al., 2020). The moving image sequences in the experiment are all those constructed by the spatial video and the standard video. The following images are selected for the experiments:

In the experiment, the subjective evaluation index and the objective evaluation index PSNR are used to evaluate the effectiveness of the two methods.

The specific calculation method of PSNR index is as follows:

The higher PSNR is, the closer the denoised image is to the original image. PSNR is defined as:

$$PSNR = 10 \log_{10} \frac{255^2}{\sum_{i=1}^c c(M/N)} dB \quad (20)$$

In the formula, M , N represent the length and width of the image respectively, and $\sum_{i=1}^c c$ represents the denoised image.

The subjective evaluation criterion is based on human visual perception. According to certain experience criteria and self-perception, the visual effect judgment is made for the blurred image, and the image quality is evaluated according to the existing evaluation scale. However, the observer must have normal vision and a certain amount of experience. Table 3 shows the commonly-used subjective evaluation scales:

In the experimental process, the motion blur of the selected image is processed, and then the motion blur parameters are restored by using the improved algorithm. The blur scale of lena.bmp is 5, and the blur angle is 7; the blur scale of signboard.bmp is 5, and the blur angle is 5.

At the same time, in order to make the experimental results more comparative, the noise is added and then the PSNR index values of the two methods are compared to determine the

Table 3 Subjective evaluation scale.

Grade	Absolute Measurement Scale	Relative Measurement Scale
5	well	Best in a group
4	better	Better than the group average
3	general	The group average
2	Worse	Worse than the group average
1	Very poor	Worst in the group

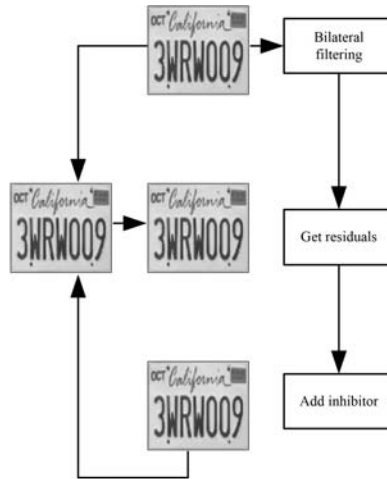


Figure 6 Experimental image preprocessing.

influence of strong noise. Before the experiment, the image preprocessing process is as follows:

3.2 Analysis of Experimental Results

Figure 7 below shows the peak signal-to-noise ratio (PSNR) index value of the proposed method and the traditional method after the enhancement of a moving image.

In Figure 7, the red curve shows the added noise. From the analysis of the figure, it can be seen that the proposed enhancement method based on the Chaos Quantum algorithm has a significantly higher PSNR value than that obtained by the traditional method. Moreover, under the influence of strong noise, the proposed method has a higher PSNR value, and with the increase of noise level, its superior performance becomes more obvious.

As can be seen from Figure 8, compared with the motion-blurred image, the proposed image enhancement method has a better processing effect, the enhanced image contrast is significantly improved, and the details are clearer. The main reason is that by means of similarity weight calculation, the region correlation judgment strategy of adaptive threshold control and Chaos Quantum algorithm are used. On the one hand, it is advantageous to learn more similar patterns to use in similarity weight calculation, so as to improve the accuracy of weight calculation; on the other hand, only the most relevant areas are used for weight calculation, rather than all areas, so the enhancement efficiency has also been greatly improved.

In practical application, there is still the situation where the original image information cannot be known, requiring several evaluation parameters to evaluate the image sharpness

after image enhancement. The basis for judging the image sharpness is given below.

Image standard deviation is a specific description of the dispersion degree of gray value relative to its average value. In general, if the image quality is better, it means that the larger the standard deviation is, the more scattered the gray level distribution of the image is. The calculation formula is:

$$std = \sqrt{\frac{1}{MN} \sum_{i=1}^M \sum_{j=1}^N (F(i, j) - u)^2} \quad (21)$$

In the above formula, M , N represent the length and width of the image respectively, and u represents the average value of the image pixels.

Information entropy measures the amount of information in an image from the perspective of information theory, which refers to the average amount of information in an image. It is an important index used to measure the quality of an image. Generally, the more information an image contains, the more entropy it has. The information entropy of image is defined as:

$$E = - \sum_{l=0}^L p(l) \log_2 p(l) \quad (22)$$

In the above formula, L represents the gray level of the image, $p(l)$ represents the probability that the gray value appears in the image l .

As can be seen from Table 4, compared with the original image, the standard deviation and information entropy of the image processed by the algorithm are significantly improved. It shows that the image quality and information quantity are guaranteed. The main reason is that the Chaos Quantum

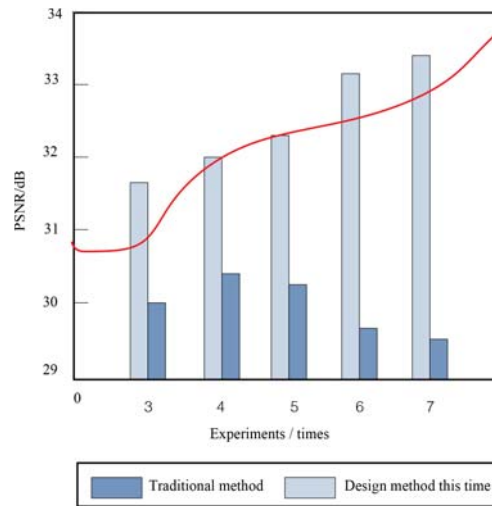


Figure 7 Comparison results of PSNR values.



(a) Motion-blurred image



(b) Enhancement effect of traditional methods



(c) Enhancement effect of the proposed method

Figure 8 Enhancement effect of blurred image.

Table 4 Evaluation indexes of different enhancement algorithms for motion-blurred images.

	Original Image	Traditional Enhancement Algorithm	Design Enhancement Algorithm
standard deviation	18.3790	30.1245	32.1021
Information entropy	5.7965	5.9412	6.2156

algorithm is used in the design algorithm, in which the regularity of chaos enables a new solution to be generated by certain iterations; The randomness prevents the the search from falling into local optimum. The ergodicity makes the final solution approach the real optimal solution with arbitrary accuracy, and improves the image quality after enhancement.

4. CONCLUDING REMARKS

The proposed method sought to address the problem of motion-blur in an image. An approach based on the Chaos Quantum algorithm was designed to enhance motion-blurred images, and achieved some promising results, with experiments proving the effectiveness of this design. Future work will be undertaken to extend and expand the research conducted for this paper. In regard to the enhancement of a moving image, the noise type involved in the image enhancement method proposed in this paper is subject to Gaussian distribution; hence, future studies will be conducted in the non-Gaussian noise environment, to establish the non-Gaussian noise distribution model and to expand the denoising method based on the Gaussian assumption. Very unclear. I can't work out the meaning here. In future research, it will be necessary to integrate multiple types of features for similarity calculation, explore the fast nonlocal fuzzy registration mechanism for multiple feature fusion, and further improve the reconstruction effect and the robustness of the algorithm.

REFERENCES

- Ahmad Khan, H., Thomas, J.B., Hardeberg, J.Y., Laligant, O. 2017. Illuminant estimation in multispectral imaging. *Journal of the Optical Society of America A*, 34, 1085.
- Amid, C., Olstedt, M., Gunnarsson, J.S., Le Lan, H., Tedengren, M. 2017. Additive effects of the herbicide glyphosate and elevated temperature on the branched coral *acroporaformosa* in NhaTrang, Vietnam. *Environmental Science and Pollution Research*, 25, 1–13.
- Bao, Y.G., Gaylord, T.K. 2018. Iterative optimization in tomographic deconvolution phase microscopy. *Journal of the Optical Society of America A*, 35, 652.
- Christoph, B., Herbert, G. 2018. Double freeform illumination design for prescribed wave fronts and irradiances. *Journal of the Optical Society of America A*, 35, 236.
- Eirik, T.B., Skjølsvæl, Kleiven, D., Patil, N., Chushkin, Y., Breiby, D.W. 2018. High-resolution coherent x-ray diffraction imaging of metal-coated polymer microspheres. *Journal of the Optical Society of America A*, 35, 7.
- Ennis, R., Schiller, F., Toscani, M., Gegenfurtner, K.R. 2018. Hyperspectral database of fruits and vegetables. *Journal of the Optical Society of America A*, 35, 256.
- Evgeny, N.B., Almas, F.S. 2017. Propagating bloch bound states with orbital angular momentum above the light line in the array of dielectric spheres. *Journal of the Optical Society of America A*, 34, 949.
- Hai, J. 2019. Automatic enhancement simulation of multi focus fuzzy feature of wavelet transform image. *Computer Simulation*, 36(11), 360–364.
- Khajavi, B., Galvez, E.J. 2017. Monstar disclinations in the polarization of singular optical beams. *Journal of the Optical Society of America A*, 34, 568.
- Laparra, V., Berardino, A., Ballé, J., Simoncelli, E.P. 2017. Perceptually optimized image rendering. *Journal of the Optical Society of America A*, 34, 1511–1525.
- Li, J.Z., Feng, X., Thierry, B. 2017. Fast and accurate three-dimensional point spread function computation for fluorescence microscopy. *Journal of the Optical Society of America A*, 34, 1029–1034.
- Maleki, E., Babashah, H., Koochi, S., Kavehvasht, Z. 2017. High-speed all-optical DNA local sequence alignment based on a three-dimensional artificial neural network. *Journal of the Optical Society of America A*, 34, 7, 1173.
- Mohammadzade, H., Ghojogh, B., Faezi, S., Shabany, M. 2017. Critical object recognition in millimeter-wave images with robustness to rotation and scale. *Journal of the Optical Society of America A*, 34, 846.
- Mohan A., Sundararajan M. 2020. Fractal Antenna – Wireless Communication New Beginning Breakthrough In Digital Era. *Acta Informatica Malaysia*, 4(1):01–06.
- Mourard, D., Bério, P., Perraut, K., Clausse, J.M., Nardetto, N., 2017. Spica. Stellar parameters and images with a cophased array: A 6T visible combiner for the chara array. *Journal of the Optical Society of America A*, 34, 37.
- Nawaz Z., Sajid A., Anwar S., Khalid H. 2019. Review Paper on Bitcoin Technology. *Information Management and Computer Science*, 2(1), 01–03.
- Ofner, J., Brenner, F., Wieland, K., Eitenberger, E., Lohninge, H. 2017. Image-based chemical structure determination. *Scientific Reports*, 7, 6832.
- Ramos, T., Jørgensen, J.S., Andreasen, J.W. 2017. Automated angular and translational tomographic alignment and application to phase-contrast imaging. *Journal of the Optical Society of America A*, 34, 1830.
- Rasid S.M.R., Hossain M.B., Hoque M.E., Arif M. and Sarder M.S.A. 2019. Modeling and Control of a Magnetic Levitation System Using an Analog Controller. *Acta Electronica Malaysia*, 3(2), 41–44.
- Somkuwar, A.S., Das, B., Vinu, R.V., Park, Y.K., Singh, R.K. 2017. Holographic imaging through a scattering layer using speckle interferometry. *Journal of the Optical Society of America A*, 34(8), 1392.
- Thiebaud, R., Lu, T.L., Chauve, T., Bernacki, M., Montagnat, M. 2017. Modelling the transport of geometrically necessary dislocations on slip systems: application to single- and multi-crystals of ice. *Modelling and Simulation in Materials Science and Engineering*, 25, 1–27.
- Yang, T., Xu, Y.G., Tian, H.H., Die, D., Dan, Y.Q. 2017. Propagation of partially coherent laguerre gaussian beams through inhomogeneous turbulent atmosphere. *Journal of the Optical Society of America A*, 34, 713–720.
- Zhang, J., Lu, S., Wang, X., Du, X., Ni, G., Liu, J. 2017. Automatic identification of fungi in microscopic leucorrhea images. *Journal of the Optical Society of America A Optics Image Science & Vision*, 34, 1484–1489.